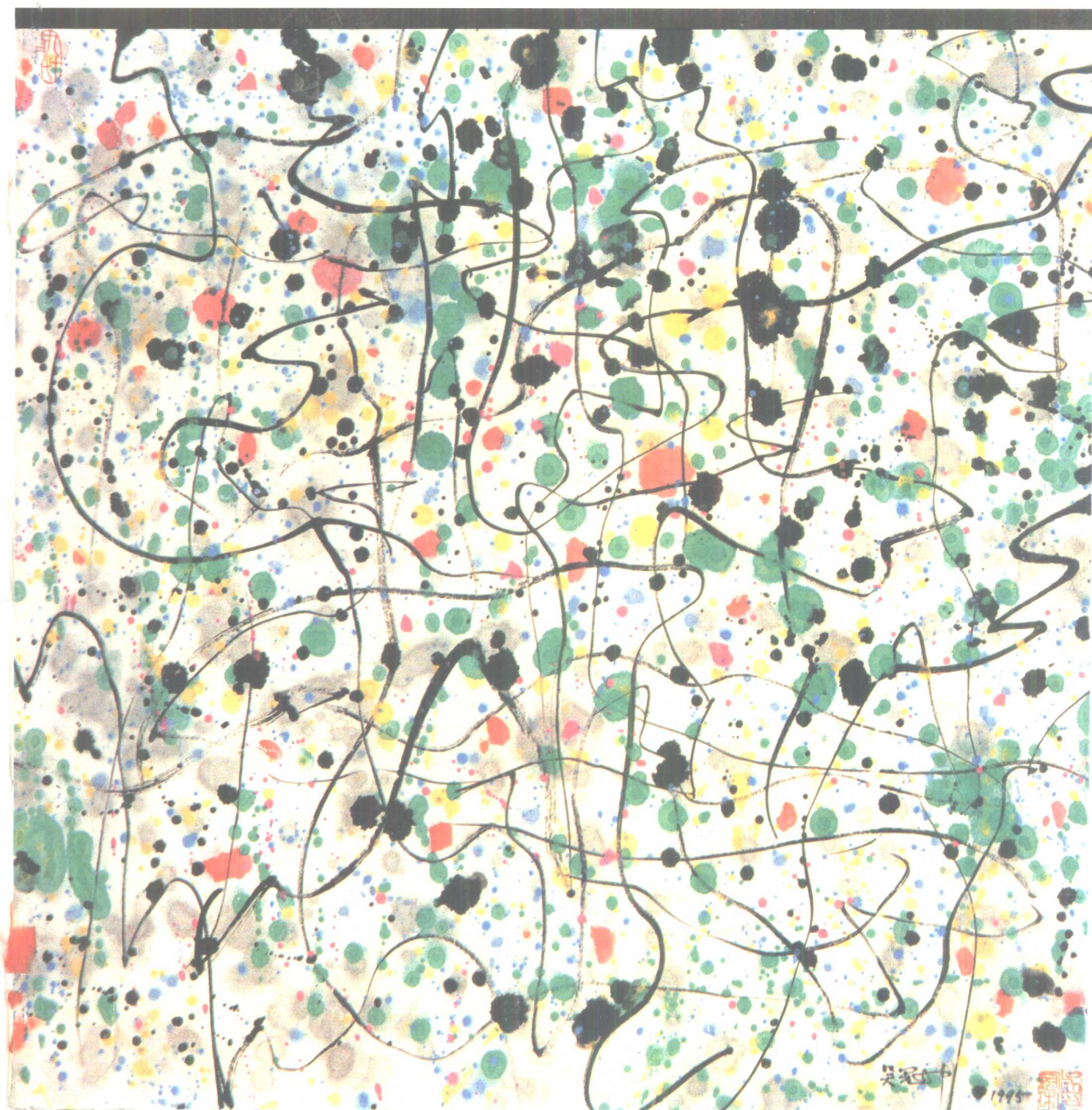


中国高等科学技术中心

CCAST—WL WORKSHOP SERIES: VOLUME 110

Nuclear Effective Interactions with
Isospin Dependence



中国高等科学技术中心

CCAST—WL WORKSHOP SERIES: VOLUME 110

Nuclear Effective Interactions with Isospin Dependence

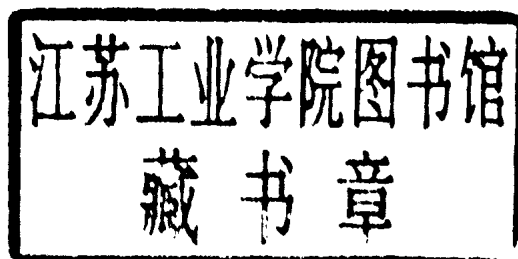
同位旋有关的有效相互作用

organized by

Zhong-yu Ma

China Institute of Atomic Energy

Beijing, P. R. China



Proceedings of

CCAST (World Laboratory) Workshop

held at

China Center of Advanced Science and Technology

Beijing, P. R. China

August 23 - 27, 1998

Printed in December 1999

Preface to the CCAST–World Laboratory Series

The China Center of Advanced Science and technology (CCAST) was established on October 17, 1986 through the strong support of World Laboratory and the Chinese Government. Its purpose is to introduce important frontier areas of science to China, to foster their growth by providing a suitable environment, and to promote free exchange of scientific information between China and other nations.

An important component of CCAST's activities is the organization of domestic and international* symposium/workshops. Each academic year we hold about 20 domestic symposium/workshops which last an average of one to two weeks each. The subjects are carefully chosen to cover advanced areas that are of particular interest to Chinese scientists. About 30–60 participants, from senior scientists to graduate students, are selected on a nationwide basis for each program. During each workshop these scientists hold daily seminars and work closely with each other.

Since 1990, CCAST has also sponsored a vigorous program for young Chinese scientists who have already made world-class contributions and are currently doing research abroad. They return to China to participate the domestic symposium/workshops, to lecture at CCAST and to collaborate with their colleagues at home. In this way, they can bring to China their own expertise, and when they go back to their institutions abroad they will be able to circulate in turn the knowledge they have acquired in China.

China is at a pivotal point in her scientific development. She is gradually emerging as an important and dynamic force in shaping the advanced science and technology of the future. This series is part of the this remarkable evolution. It records the effort, dedication, and sharing of knowledge by the Chinese scientists, at home and abroad.

T.D. Lee

* The CCAST international symposium/workshop series is published separately by Gordon and Breach Scientific Publishers.

Contents*

Preface to the series

T.D. Lee I

Nuclear Structure Derived from Realistic Nucleon-Nucleon Interactions

H. Müther 1

Renormalized Baryon Propagator in Relativistic Hartree-Fock Approximation and Effects of Self-Consistency

Shi-shu Wu, Hai-xia Zhang, Yu-jie Yao 45

✓ Hadron Structure and Vac Structure in a Hamiltonian Approach *L. M. Yang* 61

Contribution from Dirac States in a Consistent Relativistic RPA

Zhong-yu Ma 67

Modern Nucleon-Nucleon Interactions with Isospin Dependence — An Outline

Lei Li, Ping-zhi Ning 81

Strange Hadronic Matter in a Modified Quark-Meson Coupling Model

H. Q. Song, P. Wang, R. K. Su, L. L. Zhang 101

Neutron Rich Nuclei, in Density Dependent Relativistic Hartree-Fock Theory with Isovector Mesons

B. Q. Chen, Z. Y. Ma, F. Grümmer, S. Krewald 127

奇异强子物质中的重子体积效应

孙宝玺, 李磊, 宁平治, 赵恩广 137

Relativistic Mean Field Approach at Quark Level <i>Hong Shen</i>	143
Ξ^--N Interaction and Ξ^- Hypernuclei <i>Yu-hong Tan, Yan-an Luo, Ping-zhi Ning</i>	147
Hot Nuclear Matter in the Chiral σ-ω Model with Dilatons <i>Xiao-bing Zhang, Xue-qian Li, Ping-zhi Ning</i>	165
Nucleon-Pair Shell Model: the Effect of the Quadrupole n-p Force on the Collectivity of Low-Lying States <i>Yan-an Luo, Ping-Zhi Ning, Jin-Quan Chen</i>	177
Quark Condensates in Medium <i>G. X. Peng, H. C. Chiang, L. M. Zhou, X. G. Cheng</i>	189
附录	
1. 研讨会日程	211
2. 通讯录	213

· 感谢世界实验室、中国科学院、国家自然科学基金委员会、国家计委对中国高等科学技术中心的资助

Nuclear Structure derived from Realistic Nucleon-Nucleon Interactions

H. Mütter

Institut für Theoretische Physik,
Universität Tübingen, Tübingen, Germany

August 17, 1999

Abstract

Correlations in the nuclear wave-function beyond the mean-field or Hartree-Fock approximation are very important to describe basic properties of nuclear structure. Attempts are made to explore details of these correlations and their sensitivity to the underlying nucleon-nucleon interaction. Special attention is paid to the attempts to investigate these correlations in exclusive nucleon knock-out experiments induced by electron scattering. Another important issue of nuclear structure physics is the role of relativistic effects as contained in phenomenological mean field models. Predictions for these relativistic effects based on realistic meson-exchange interactions are discussed. The sensitivity of various nuclear structure observables on these relativistic features are investigated. The report includes the discussion of nuclear matter as well as finite nuclei.

1 Introduction

Nuclei are a very intriguing object to explore the theory of quantum-many-body systems. One of the reasons is that realistic wave functions of nuclear systems must exhibit strong two-particle correlations. This can be demonstrated in a little ‘theoretical experiment’: Assuming a realistic model for the nucleon-nucleon (NN) interaction[1, 2, 3, 4, 5], this means an interaction which reproduces the empirical data of NN scattering below the pion threshold, one may calculate the energy of nuclear matter within the mean field or Hartree-Fock approximation. Results of such a calculation are listed in the fourth row of table 1, which is labeled $\langle E \rangle_{\text{HF}}$. One finds that all these interactions yield a positive value for the energy per nucleon, which means that nuclear matter as well as all nuclei would be unbound. Only after the effects of two-body correlations are included, one obtains a value which is in rough agreement with the empirical value of -16 MeV per nucleon. This demonstrates that nuclear correlations are indispensable to describe the structure of nuclei.

The different interaction models all reproduce the same empirical NN scattering phase shifts. This is true in particular for the modern NN interactions: the charge-dependent Bonn potential (CDB)[1], the Argonne V18 (ArgV18)[2] and the Nijmegen interaction (Nijm1)[3], which all yield an excellent fit of the same phase shifts. Nevertheless, they predict quite different results for the energy calculated in the mean field approximation. What is the

	CDBonn	ArV18	Nijm1	Nijm2	A	B	C	Reid
$\langle E \rangle$	-17.11	-15.85	-15.82	-13.93	-16.32	-15.32	-14.40	-12.47
$\langle V \rangle$	-53.34	-62.92	-55.08	-61.94	-52.44	-53.03	-54.95	-61.51
$\langle T \rangle$	36.23	47.07	39.26	48.01	36.12	37.71	40.55	49.04
$\langle V_\pi \rangle$	-22.30	-40.35	-28.98	-28.97	-12.48	-26.87	-45.74	-27.37
$\langle E \rangle_{\text{HF}}$	4.64	30.34	12.08	36.871	7.02	10.07	29.56	176.25
$P_D [\%]$	4.83	5.78	5.66	5.64	4.38	4.99	5.62	6.47

Table 1: Energies calculated for nuclear matter with Fermi momentum $k_F = 1.36 \text{ fm}^{-1}$. Results are listed for the energy per nucleon calculated in BHF ($\langle E \rangle$) and Hartree-Fock ($\langle E \rangle_{\text{HF}}$) approximation. Furthermore the expectation value for the NN interaction $\langle V \rangle$, the kinetic energy $\langle T_{\text{Kin}} \rangle$ and the one-pion-exchange term $\langle V_\pi \rangle$ are listed. For completeness we also give the D-state probability calculated for the deuteron P_D . Results are presented for the charge-dependent Bonn (CDBonn) [1], the Argonne V18 (ArV18) [2] and two Nijmegen (Nijm1, Nijm2) [3] interactions. For a comparison results are also given for three older versions of the Bonn interaction (A,B,C) [4] and the Reid soft core potential [5], which is supplemented in partial waves in which it is not defined by the OBE C potential. All energies are given in MeV per nucleon.

origin of this difference? In order to answer this question we will discuss in the very first part of this lecture some differences in these modern version of realistic NN interactions in the first section after this introduction. We will pay special attention to the role of non-localities in the NN interactions and demonstrate that the neglect of non-local contributions has some non-negligible effects even for the description of the deuteron.

In the third section we will discuss some main features of correlations in nuclear matter. This includes a short introduction into Brueckner theory, the Brueckner-Hartree-Fock (BHF) approach and an analysis of the differences derived from the various interactions. After we have established the importance of nuclear correlations within the theoretical framework, we will discuss possibilities to establish their effects in experiments. A lot of effort has been made to investigate the effects of nuclear correlations in exclusive nucleon knock-out experiments induced by inelastic electron scattering. A status report on these efforts will be presented in section 4.

Including the effects of correlations into the calculation yields a significant improvement in the calculation of binding properties of nuclear matter. However, a typical discrepancy remains for the study of nuclear matter. This is a very old problem and has been called the problem of the “Coester band” of nuclear matter [6]: Realistic NN interactions which essentially reproduce the binding energy of nuclear matter lead to a saturation density which is about twice the empirical value. Other interactions, which predict about the correct saturation density yield, a value for the binding energy which is about a 5 MeV smaller than the experimental value of -16 MeV per nucleon. A very similar feature is also obtained in calculating the bulk properties of finite nuclei[7]. A possible way out of this problem is to introduce three-nucleon forces with parameters adjusted to reproduce the experimental data for the ground state[8]. The obvious disadvantage of this approach is of course that the many-body calculation is not free of adjustable parameters as long as one cannot deduce these many-nucleon forces from an underlying theory.

Attempts have been made to consider sub-nucleonic degrees of freedom within the many-

body theory of finite nuclei and nuclear matter. As an example we mention various investigations in which the excitations of the interacting nucleons to the $\Delta(3,3)$ resonance or other excitation modes were considered explicitly. The dynamic treatment of the excitation modes can be described in terms of an effective NN interaction which is modified in the nuclear medium [9] plus effective many-nucleon forces involving three and more nucleons [10]. Also the consideration of these sub-nucleonic degrees of freedom has a considerable effect on the description of the saturation point of nuclear matter as well as on the evaluation of bulk properties for finite nuclei. However, similar to the study of many-nucleon correlations one observes also in this case a modification of the predicted properties essentially along the Coester band, which means that a very similar result could be obtained by employing a different phase-shift equivalent NN interaction rather than including these sub-nucleonic degrees of freedom [11].

A possible solution of the long standing problem to derive ground state properties of nuclear systems from realistic NN forces has been shown by the Dirac-Brueckner-Hartree-Fock (DBHF) approach applied to nuclear matter. The important ingredient of this approach, which moves the calculated saturation point for nuclear matter off the Coester band, is the consideration of the various components in the relativistic self energy of the nucleon in the nuclear medium. A strong attractive part (around -300 MeV), which transforms like a scalar under a Lorentz transformation and mainly originates from the exchange of the scalar σ meson in realistic One-Boson-Exchange (OBE) models [4] of the NN interaction, is partly compensated by a repulsive component which transforms like a time-like component of a Lorentz vector and reflects the repulsion due to the ω meson exchange. The effects of this two contributions cancel each other to a large extent in calculating the single-particle energy of the nucleon, which is small (-40 MeV) on the scale of the mass of the nucleon. Inserting the nucleon self-energy in a Dirac equation for the nucleon, however, the strong scalar part of the self-energy yields a strong enhancement of the small component in the Dirac spinor of the nucleon in the medium as compared to the vacuum. This modification of the Dirac spinors in the nuclear medium leads to modified matrix elements for the OBE interaction. It is this density dependence of the nucleon Dirac spinors and the resulting medium dependence of the NN interaction which moves the saturation point calculated for nuclear matter off the Coester band in such a way, that the empirical values for the energy per nucleon and the saturation density can be reproduced without the necessity to adjust any parameter or to introduce many-nucleon forces as we will see in section 5.

This success of the DBHF approach in nuclear matter gives rise to the hope that a DBHF calculation for finite nuclei may also provide a satisfactory description of the ground state properties. The self-consistency requirement of the DBHF approach is quite involved and we will discuss some techniques to solve these problems in section 6.

The self-consistency problem of DBHF calculations for finite nuclei is of course even more involved than for nuclear matter. It can be simplified in terms of a local density approximation (LDA). In section 5 we will present a LDA in which the effects of correlations are determined in nuclear matter at various densities leading to an effective meson-exchange model with density dependent coupling constants. The density dependence of the coupling constants reflects the density dependence of the correlation effects. Assuming that the correlation effects in finite nuclei can be approximated by those in nuclear matter at the same density, one obtains an approximation to the DBHF by solving Dirac-Hartree-Fock equations with a density-dependent meson exchange for finite nuclei. It turns out that the results of this LDA are similar to those of a DBHF calculation for finite nuclei.

The LDA can furthermore be used to explore relativistic effects on observables beyond the binding energy and the radius of nuclei. As examples we will discuss the spin-orbit splitting in the single-particle spectrum, the energy dependence of the optical model for nucleon - nucleus scattering, and the response functions for exclusive ($e, e'p$) reactions in section 7. Some concluding remarks are made in the final section 8.

2 Realistic Interactions and the Deuteron

During the past few years, considerable progress has been made in constructing realistic models for the nucleon-nucleon (NN) interaction. Several of these models describe an identical data base of NN scattering data with a χ^2 per datum ≈ 1 [3, 2, 1], meaning in turn that the on-shell matrix elements of the NN transition matrix T are essentially equal. This does, however, not imply that the models for the NN interaction underlying these descriptions are identical. Moreover, the off-shell properties of each potential may be rather different. All models for the NN interaction V include a one-pion exchange (OPE) term, using essentially the same πNN coupling constant, and account for the difference between the masses of the charged (π_{\pm}) and neutral (π_0) pion. However, even this long range part of the NN interaction, which is believed to be well understood, is treated quite differently in these models.

The CD-Bonn potential is based consistently upon relativistic meson field theory [1]. Meson-exchange Feynman diagrams are typically nonlocal expressions that are represented in momentum-space in analytic form. As an example we present the expression for the One-Pion-Exchange contribution to the NN interaction of two nucleons in the 3S_1 channel, in plane wave states with momenta k and k' for the initial and final state, respectively

$$\langle k' | V_{SS}^{\pi} | k \rangle = -\frac{g_{\pi}^2}{4\pi} \frac{1}{2\pi M^2} \sqrt{\frac{M^2}{E_k E_{k'}}} \int_{-1}^1 d\cos\theta \left(\frac{\Lambda^2 - m_{\pi}^2}{\Lambda^2 + q^2} \right)^2 \frac{k' k \cos\theta - (E_k E_{k'} - M^2)}{q^2 + m_{\pi}^2}, \quad (1)$$

where q^2 denotes the momentum transfer,

$$\begin{aligned} q^2 &= (\mathbf{k} - \mathbf{k}')^2 = k^2 + k'^2 - 2kk' \cos\theta, \\ E_k &= \sqrt{k^2 + M^2}, \end{aligned} \quad (2)$$

and m_{π} is the mass of the pion (note that in order to shorten the notation we ignore in these equations the charge dependence of m_{π} and the nucleon mass M); Λ stands for the cut-off parameter, which was chosen to be $\Lambda = 1.7$ GeV [1]. Results for such matrix elements as a function of k , keeping $k' = 95$ MeV/c fixed, are displayed in Fig. 1[12].

If we introduce now the nonrelativistic approximation for

$$E_k E_{k'} - M^2 \approx \frac{1}{2}k^2 + \frac{1}{2}k'^2, \quad (3)$$

we obtain (ignoring the form factor $(\Lambda^2 - m_{\pi}^2)/(\Lambda^2 + q^2)$ and the relativistic square-root factors)

$$\langle k' | V_{SS}^{\pi} | k \rangle_{\text{local}} = -\frac{g_{\pi}^2}{4\pi} \frac{1}{2\pi M^2} \int_{-1}^1 d\cos\theta \left(\frac{m_{\pi}^2}{2(q^2 + m_{\pi}^2)} - \frac{1}{2} \right). \quad (4)$$

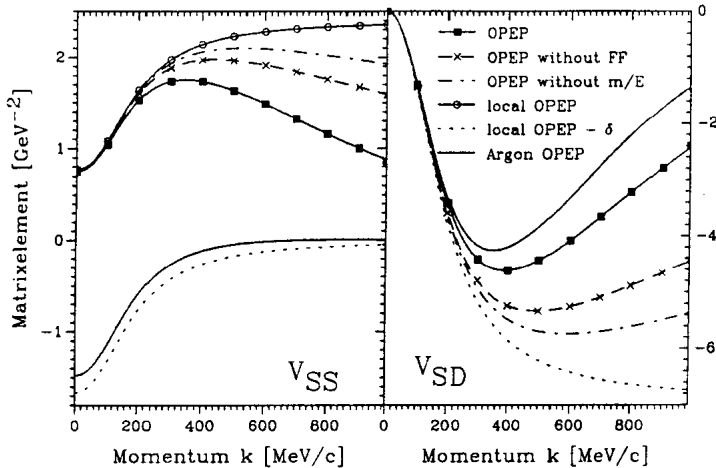


Figure 1: Plane-wave matrix elements of the one-pion-exchange potential (OPEP) using various approximations. As an example, the matrix elements in momentum space $\langle k'|V|k \rangle$ are shown as functions of k for a fixed value of $k' = 95$ MeV/c. The left part of the figure exhibits matrix elements for the partial waves 3S_1 - 3S_1 , while the right part shows the tensor component in the 3S_1 - 3D_1 channel with k referring to the momentum in the 3D_1 partial wave.

This can be viewed as the local approximation to the OPE since the matrix element depends on the momentum transfer q^2 , only. It can easily be transformed into the configuration-space representation, resulting in a Yukawa term plus a δ function, which originates from the Fourier transform of the constant $1/2$ in Eq. (4). The various steps leading to this result are shown in Fig. 1. It is obvious from this figure that all of the steps leading to the local expression (4) are not really justified for momenta k around and above 200 MeV, a region of relative momenta which is of importance in the deuteron wave function. This is true for the matrix elements V_{SS} as well as V_{SD} . It is remarkable that the regularization of the local OPE by the local Gaussian form factor introduced in the Argonne V_{18} potential leads to matrix elements in the SD -channel which are close to those derived from the relativistic expression of the Bonn potential. This is not the case in the SS channel, where the removal of the δ function term is very significant. This comparison of the various approximations to the OPE part of the NN interaction demonstrates that even this long range part of the NN interaction is by no means settled. The local approximation and the regularization by form factors have a significant effect.

The description of the short-range part is also different in these models. The NN potential Nijm-II [3] is a purely local potential in the sense that it uses the local form of the OPE potential for the long-range part and parameterizes the contributions of medium and short-range in terms of local functions (depending only on the relative displacement between the two interacting nucleons) multiplied by a set of spin-isospin operators. The same is true for the Argonne V_{18} potential [2]. The NN potential denoted by Nijm-I [3] uses also the local form of OPE but includes a \mathbf{p}^2 term in the medium- and short-range central-force (see Eq. (13) of Ref. [3]) which may be interpreted as a non-local contribution to the central

Pot.	T_S [MeV]	T_D [MeV]	V_{SS} [MeV]	V_{DD} [MeV]	V_{SD} [MeV]	P_D [%]
CD-Bonn	9.79	5.69	-4.77	1.34	-14.27	4.83
Argon V_{18}	11.31	8.57	-3.96	0.77	-18.94	5.78
Nijm I	9.66	7.91	-1.35	2.37	-20.82	5.66
Nijm II	12.11	8.10	-5.40	0.59	-17.63	5.64

Table 2: Contributions to the kinetic and potential energy of the deuteron originating from the 3S_1 and 3D_1 parts of the wave function as defined in Eq. 5. Results are listed for the charge-dependent Bonn potential (CD-Bonn [1]), the Argonne V_{18} [2], the Nijmegen potentials Nijm I and Nijm II [3]. The last column of this Table shows the calculated D -state probabilities of the deuteron.

force. The CD-Bonn potential is based consistently upon relativistic meson field theory [4]. Meson-exchange Feynman diagrams are typically nonlocal expressions that are represented in momentum-space in analytic form. It has been shown [1] that ignoring the non-localities in the OPE part leads to a larger tensor component in the bare potential.

By construction, all realistic NN potentials reproduce the experimental value for the energy of the deuteron of -2.224 MeV. However, the various contributions to the total deuteron energy originating from kinetic energy and potential energy in the 3S_1 and 3D_1 partial waves of relative motion,

$$\begin{aligned}
E &= \langle \Psi_S | T | \Psi_S \rangle + \langle \Psi_D | T | \Psi_D \rangle + \langle \Psi_S | V | \Psi_S \rangle + \langle \Psi_D | V | \Psi_D \rangle + 2\langle \Psi_S | V | \Psi_D \rangle \\
&= T_S + T_D + V_{SS} + V_{DD} + V_{SD},
\end{aligned} \tag{5}$$

exhibit quite different results. This can be seen from the numbers listed in Table 2. In this table, we display the various contributions to the deuteron binding energy employing the four potentials introduced above.

The kinetic energies are significantly larger for the local potentials V_{18} and Nijm II than for the two interaction models CD-Bonn and Nijm I which contain non-local terms. The corresponding differences in the S -wave functions can be seen in Fig. 2.

Comparing the contributions to the potential energy, displayed in Table 2, one finds large differences particularly for the tensor contribution V_{SD} . The dominant part of this tensor contribution should originate from the tensor component of the one-pion-exchange potential which we discussed above.

In summary, although the modern NN potentials yield the same binding energy for the deuteron, there are significant differences in the contributions to both the kinetic and potential energy in the various partial waves. Speaking in general terms, these differences can be traced back to off-shell differences between the potentials. In particular it is the inclusion of non-local contributions in the long-rang (π exchange) as well as short-range part of the NN interaction, which is responsible for these differences.

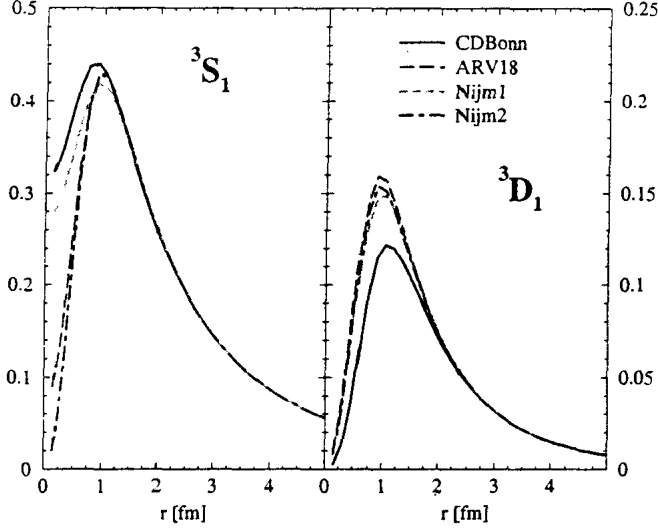


Figure 2: Wave function for the deuteron (3S_1 and 3D_1) calculated for different realistic interactions.

3 Correlations in Nuclear Matter

The necessity to incorporate correlations beyond the Hartree-Fock approximation in the many-body wavefunction of nuclear systems has been demonstrated already in the introduction, discussing the results obtained for the binding energy of nuclear matter using the Hartree-Fock approximation (see Table 1). One way to account for nucleon-nucleon (NN) correlations is to employ the lowest Brueckner theory or hole-line expansion, which in lowest order yields the Brueckner-Hartree-Fock (BHF) approach. The central equation of the BHF approximation is the Bethe-Goldstone equation, which defines an effective interaction G for two nucleons in nuclear matter occupying the plane wave states i and j by

$$G|ij\rangle = V|ij\rangle + V \frac{Q}{\epsilon_i + \epsilon_j - H_0} G|ij\rangle. \quad (6)$$

Here and in the following V stands for the bare NN interaction, Q denotes the Pauli operator, which prevents of the interacting nucleons into intermediate states with momenta below the Fermi momentum k_F , H_0 defines the spectrum of intermediate two-particle states and the BHF single-particle energies are defined by

$$\epsilon_i = \frac{\hbar^2 k_i^2}{2M} + \int_0^{k_F} d^3 k_j \langle ij|G|ij\rangle, \quad (7)$$

as the sum of the kinetic energy of a free nucleon with mass M and momentum k_i and the potential energy. The single particle potential corresponds to the Hartree-Fock approximation but calculated in terms of the effective interaction G rather than the bare interaction V . Also the total energy of the system is calculated in a similar way containing the kinetic

energy per nucleon of a free Fermi gas

$$\frac{T_{FG}}{A} = \frac{3}{5} \frac{\hbar^2 k_F^2}{2M}, \quad (8)$$

and the potential energy calculated in the Hartree-Fock approximation replacing V by the effective interaction G (For a more detailed description see e.g. [13]). This means that the BHF approach considers a model wave function, which is just the uncorrelated wave function of a free Fermi gas and all information about correlations are hidden in the effective interaction G . Since this effective interaction is constructed such that G applied to the uncorrelated two-body wave function yields the same result as the bare interaction V acting on the correlated wave function

$$G|ij\rangle = V|ij\rangle_{\text{corr.}}, \quad (9)$$

the comparison of this equation with (6) allows the definition of the correlated two-nucleon wave function as

$$|ij\rangle_{\text{corr.}} = |ij\rangle + \frac{Q}{\epsilon_i + \epsilon_j - H_0} G|ij\rangle. \quad (10)$$

This representation demonstrates that the correlated wave function contains the uncorrelated one plus the so-called defect function, which in this approach should drop to zero for relative distances between the two nucleons, which are larger than the healing distance.

The BHF approach yields the total energy of the system including effects of correlations. Since, however, it does not provide the correlated many-body wave function, one does not obtain any information about e.g. the expectation value for the kinetic energy using this correlated many-body state. To obtain such information one can use the Hellmann-Feynman theorem, which may be formulated as follows: Assume that one splits the total Hamiltonian into

$$H = H_0 + \Delta V \quad (11)$$

and defines a Hamiltonian depending on a parameter λ by

$$H(\lambda) = H_0 + \lambda \Delta V. \quad (12)$$

If E_λ defines the eigenvalue of

$$H(\lambda)|\Psi_\lambda\rangle = E_\lambda|\Psi_\lambda\rangle \quad (13)$$

the expectation value of ΔV calculated for the eigenstates of the original Hamiltonian $H = H(1)$ is given as

$$\langle \Psi | \Delta V | \Psi \rangle = \left. \frac{\partial E_\lambda}{\partial \lambda} \right|_{\lambda=1}. \quad (14)$$

The BHF approximation can be used to evaluate the energies E_λ , which also leads to the expectation value $\langle \Psi | \Delta V | \Psi \rangle$ employing this eq.(14). In the present work we are going to apply the Hellmann-Feynman theorem to determine the expectation value of the kinetic energy and of the one-pion-exchange term $\Delta V = V_\pi$ contained in the different interactions.

First differences in the prediction of nuclear properties obtained from the modern interactions are displayed in table 1 which contains various expectation values calculated for nuclear matter at the empirical saturation density, which corresponds to a Fermi momentum

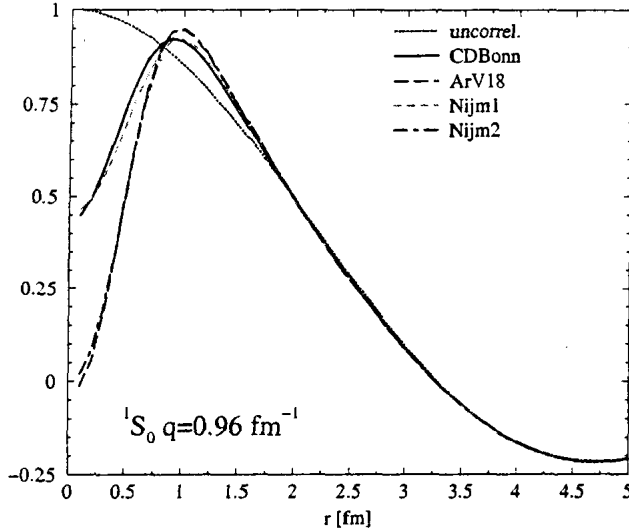


Figure 3: Correlated wave functions $|ij\rangle_{\text{corr.}}$ as defined in (10) as a function of the relative distance for the 1S_0 partial wave. Results are shown for a pair of nucleons in nuclear matter at empirical saturation density, which heal to an uncorrelated two-nucleon wave function with momentum $q = 0.96 \text{ fm}^{-1}$ at larger distances. The curves are labeled by the interactions, which were considered.

k_F of 1.36 fm^{-1} . The most striking indication for the importance of nuclear correlations beyond the mean field approximation may be obtained from the comparison of the energy per nucleon calculated in the mean-field or Hartree-Fock (HF) approximation. All energies per nucleon calculated in the (HF) approximation are positive, therefore far away from the empirical value of -16 MeV . Only after inclusion of NN correlations in the BHF approximation results are obtained which are close to the experiment. While the HF energies range from 4.6 MeV in the case of CDBonn to 36.9 MeV for Nijm2, rather similar results are obtained in the BHF approximations. This demonstrates that the effect of correlations is quite different for the different interactions considered. However it is worth noting that all these modern interactions are much “softer” than e.g. the old Reid soft-core potential[5] in the sense that the HF result obtained for the Reid potential (176 MeV) is much more repulsive.

Another measure for the correlations is the enhancement of the kinetic energy calculated for the correlated wave function as compared to the mean field result which is identical to T_{FG} , the energy per particle of the free Fermi gas. At the empirical density this value for T_{FG} is 23 MeV per nucleon. One finds that correlations yield an enhancement for this by a factor which ranges from 1.57 in the case of CDBonn to 2.09 for Nijm1. It is remarkable that the effects of correlations, measured in terms of the enhancement of the kinetic energy or looking at the difference between the HF and BHF energies, are significantly smaller for the interactions CDBonn and Nijm1, which contain non-local terms.

The table 1 also lists the expectation value for the pion-exchange contribution V_π to the two-body interaction. Here one should note that the expectation value of V_π calculated in

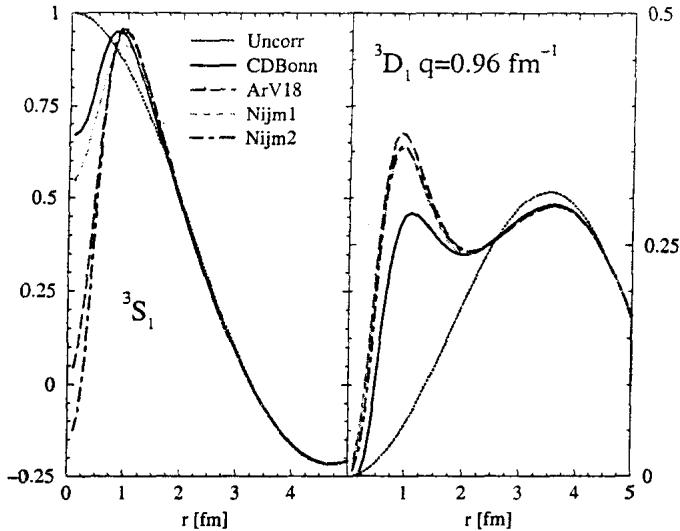


Figure 4: Correlated wave functions as a function of the relative distance for the 3S_1 and 3D_1 partial waves. Further details see Fig. 3.

the HF approximation is about 15 MeV almost independent of the interaction considered. So it is repulsive and completely due to the Fock exchange term. If, however, the expectation value for V_π is evaluated for the correlated wave function, one obtains rather attractive contributions ranging from -22.30 MeV per nucleon (CDBonn) to -40.35 MeV (ArV18). This expectation value is correlated to the strength of the tensor force or the D-state probability P_D calculated for the deuteron (see table 1 as well). Interactions with larger P_D , like the ArV18, yield larger values for $\langle V_\pi \rangle$. For a further support of this argument we also give the results for three different version of charge-independent Bonn potentials A, B and C, defined in [4]. All this demonstrates that pionic and tensor correlations are very important to describe the binding properties of nuclei. In fact, the gain in binding energy due to correlations from V_π alone is almost sufficient to explain the difference between the HF and BHF energies.

Inspecting the expectation values for the kinetic energies we observe a feature very similar to the one observed for the deuteron: the local interactions, ArV18 and Nijm2, yield larger kinetic energies than CDBonn and Nijm1, which contain nonlocal terms. This is independent of the density considered.

A different point of view on nuclear correlations may be obtained from inspecting the relative wave functions for a correlated pair $|ij\rangle_{\text{corr}}$, defined in (10). Results for such correlated wave functions for a pair of nucleons in nuclear matter at empirical saturation density are displayed in Figs 3 and 4. As an example we consider wave functions which “heal” at larger relative distances to an uncorrelated two-nucleon wave function with momentum $q = 0.96 \text{ fm}^{-1}$ calculated at a corresponding average value for the starting energy.

Fig. 3 shows relative wave functions for the partial wave 1S_0 . One observes the typical features: a reduction of the amplitude as compared to the uncorrelated wave function for relative smaller than 0.5 fm, reflecting the repulsive core of the NN interaction, an enhance-

ment for distances between ≈ 0.7 fm and 1.7 fm, which is due to the attractive components at medium range, and the healing to the uncorrelated wave function at large r . One finds that the reduction at short short distances is much weaker for the interactions CDBonn and Nijm1 than for the other two. This is in agreement with the discussion of the kinetic energies and the difference between HF and BHF energies (see table 1). The nonlocal interactions CDBonn and Nijm1 are able to fit the NN scattering phase shifts with a softer central core than the local interactions.

Very similar features are also observed in the 3S_1 partial wave displayed in the left half of Fig. 4. For the 3D_1 partial wave, shown in the right part of Fig. 4, one observes a different behavior: All NN interactions yield an enhancement of the correlated wave function at $r \approx 1$ fm. This enhancement is due to the tensor correlations, which couples the partial waves 3S_1 and 3D_1 . This enhancement is stronger for the interactions ArV18, Nijm1 and Nijm2 than for the CDBonn potential. Note that the former potential contain a pure nonrelativistic, local one-pion-exchange term, while the CDBonn contains a relativistic, nonlocal pion-exchange contribution. See also the discussion of the wavefunction for the deuteron in the preceeding section.

4 Correlations in Nucleon Knock-out Experiments

4.1 Exclusive ($e, e'p$) Reactions

The uncorrelated Hartree-Fock state of nuclear matter is given as a Slater determinant of plane waves, in which all states with momenta k smaller than the Fermi momentum k_F are occupied, while all others are completely unoccupied. Correlation in the wave function beyond the mean field approach will lead to occupation of states with k larger than k_F . Therefore correlations should be reflected in an enhancement of the momentum distribution at high momenta. We have observed this feature already in the preceeding section, discussing the enhancement of the kinetic energy as compared to the one of the free Fermi gas. Indeed, microscopic calculations exhibit such an enhancement for nuclear matter as well as for finite nuclei[15, 16]. One could try to measure this momentum distribution by means of exclusive ($e, e'p$) reactions at low missing energies, such that residual nucleus remains in the ground state or other well defined bound state. From the momentum transfer q of the scattered electron and the momentum p of the outgoing nucleon one can calculate the momentum of the nucleus before the absorption of the photon and therefore obtain direct information on the momentum distribution of the nucleons inside the nucleus.

This idea, however, suffers from a little inaccuracy. To demonstrate this we write the momentum distribution $n(k)$ representing the ground state wave function of the target nucleus by Ψ_A , denoting the creation (annihilation) operator for a nucleon with momentum k by a_k^\dagger (a_k), as

$$\begin{aligned}
 n(k) &= \langle \Psi | a_k^\dagger a_k | \Psi \rangle \\
 &= \int_0^\infty dE \langle \Psi | a_k^\dagger | \Phi_{A-1}(E) \rangle \langle \Phi_{A-1}(E) | a_k | \Psi \rangle \\
 &= \int_0^\infty dE S(k, E) \\
 \text{with } S(k, E) &= \left| \langle \Psi | a_k^\dagger | \Phi_{A-1}(E) \rangle \right|^2.
 \end{aligned}$$

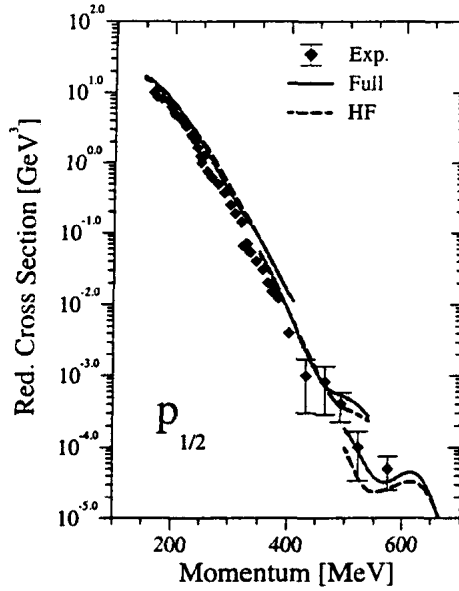


Figure 5: Reduced cross section for the $^{16}\text{O}(e, e'p)^{15}\text{N}$ reaction leading to the ground state ($1/2^-$) of ^{15}N in the kinematical conditions considered in the experiment at MAMI (Mainz) [17]. Results for the mean-field description (HF) and the fully correlated spectral function (Full) are presented.

In the second line of this equation we have inserted the complete set of eigenstates for the residual nucleus with $A - 1$ nucleons and excitation energy E . Therefore, if one performs an exclusive $(e, e'p)$ experiment leading to the residual nucleus in its ground state, one does not probe the momentum distribution but the spectral function at an energy $E = 0$. While the total momentum distribution exhibits the enhancement at high momenta discussed above, the spectral function at small energies does not have this feature[15] and the momentum distribution extracted from such experiments is very similar to the one derived from Hartree-Fock wave functions.

This is demonstrated by Figure 5, which compares experimental data of $(e, e'p)$ experiments on ^{16}O leading to the ground state of the residual nucleus ^{15}N , which were performed at MAMI in Mainz[17], with theoretical calculations[18]. The calculation account for the final state interaction of the outgoing nucleon with the residual nucleus by means of a relativistic optical potential. One finds that the spectral function calculated with inclusion of correlation yields the same shape as the corresponding Hartree-Fock approximation. The only difference being the global normalization: the spectroscopic factor.